Optimal configuration of heat engines for maximum efficiency with generalized radiative heat transfer law

Lingen Chen*, Hanjiang Song, Fengrui Sun, and Shengbing Wang
Postgraduate School, Naval University of Engineering,
Wuhan 430033, P.R. China
**e-mail: lgchenna@yahoo.com, lingenchen@hotmail.com,*
Fax: 0086-27-83638709 Tel: 0086-27-83615046.

Recibido el 24 de noviembre de 2008; aceptado el 7 de diciembre de 2009

Optimal configuration of a class of endoreversible heat engines with generalized radiative heat transfer law [$q \propto \Delta(T^n)$] has been determined by this paper. The optimal cycle that maximizes the efficiency of the engines with fixed input energy has been obtained using optimal-control theory, and the differential equations are solved by Taylor series expansion. It is shown that the optimal cycle for maximum efficiency has eight branches including two isothermal branches, four maximum-efficiency branches and two adiabatic branches. The interval of each branch has been obtained, as well as the solutions of the temperatures of heat reservoirs and working fluid. Numerical examples are given for the optimal configurations with $n=-1$, n=1, n=2, n=3 and n=4, respectively. The results obtained are compared with each other and with those results obtained for maximum power output.

Keywords: Generalized radiative heat transfer law; endoreversible heat engine; maximum efficiency; optimal configuration; finite time thermodynamics; generalized thermodynamic optimization.

En este artículo se determina la configuración óptima de una clase de motor térmico endoreversible con la ley generalizada de transferencia de claro radiativa [$q \propto \Delta(T^n)$]. El ciclo óptimo que maximiza la eficiencia de los motores con una entrada de energía dada se obtiene usando la teoría del control óptimo y las ecuaciones diferenciales son resueltas mediante la expanción en series de Taylor. Se muestra que el ciclo óptimo para máxima eficiencia tiene ocho ramas, incluyendo dos ramas isotérmicas, cuatro de máxima eficiencia y dos adiabáticas. Se muestra el intervalo para cada rama, así como la temperatura del recipiente calorífico y del fluido de trabajo. Los ejemplo numéricos se muestran para la configuración óptima con $n=-1$, n=1, n=2, n=3 y n=4. Los resultado obtenidos son comparados unos con otros, y con éstos se obtiene la potencia máxima de salida.

Descriptores: Leyes de transferencia de calor; motores endoreversibles; máxima eficiencia; configuración óptima; termodinámica de tiempos finitos.

PACS: 05.70.-a

1. Introduction

There are two standard problems in finite time thermodynamics: One is to determine the objective function limits and the relations between objective functions for the given thermodynamic system, and another is to determine the optimal thermodynamic process for the given optimization objectives [1-23]. Gutowicz-Krusion *et al.* [24] proved that in all acceptable cycles, an endoreversible Carnot cycle can produce maximum power, *i.e.* the Curzon-Ahlborn (CA) cycle [25] is the optimal configuration with only First and Second Law constraints. Rubin [26,27] analyzed the optimal configurations of endoreversible heat engines with Newton's heat transfer law [$q \propto \Delta$(T)] and different constraints, and derived the optimal configuration of the engines. The optimal configuration with fixed duration for maximum power output is a six-branch cycle, and the optimal configuration with fixed energy input for maximum efficiency is an eight-branch cycle [26]. The results were extended to a class of heat engines with fixed compression ratio, and an optimal eight-branch cycle configuration of the engines for maximum power output was derived [27]. Since then, many researchers have found various optimal configurations for various systems and devices using optimal- control theory in the last three decades.

In general, heat transfer is not necessarily linear and also obeys other laws; heat transfer law has significant influence on the configuration and performance of heat engine cycles [28-37]. Song *et al.* [38,39] and Li *et al* [40] determined the optimal configurations of endoreversible heat engines for maximum efficiency objective and maximum power output objective with linear phenomenological heat transfer law [$q \propto \Delta(T^{-1})$] [38,40] and those for maximum power output objective [39] with radiative heat transfer law [$q \propto \Delta$(T^4)]. In this paper, based on Refs. 26 and 38, the optimal configuration of endoreversible heat engines for maximum efficiency objective is obtained with fixed duration and a universal heat transfer law, *i.e.* generalized radiative heat transfer [$q \propto \Delta(T^n)$] in the heat transfer processes between working fluid and heat reservoirs. The generalized radiative heat transfer law [$q \propto \Delta(T^n)$] includes some special cases. When $n=1$, the heat transfer obeys Newtonian law; when $n=-1$, the heat transfer obeys linear phenomenological law used in irreversible thermodynamics, in which case the heat transfer coefficients are the so-called kinetic coefficients by Callen [41], and they should be negative; when n=2, the heat transfer is applicable to radiation propagated along a one-dimensional transmission line [28,29], and the heat transfer coefficient in this case is equal

to [$\pi^2\ k^2$/6h], where h is the Planck's constant and k is the Stefan-Boltzmann constant; when n=3, the heat transfer is applicable to radiation propagated along a two-dimensional surface [28,29]; when $n = 4$, the heat transfer obeys radiative law if all the bodies are black, and the heat transfer coefficient in this case is related to the Stefan-Boltzmann constant. The optimal cycles that maximize the efficiency of the engines are obtained using optimal-control theory. It is shown that the optimal cycle for maximum efficiency has eight branches including two isothermal branches, four maximum-efficiency branches and two adiabatic branches. The interval of each branch has been obtained, as well as the solutions of the temperatures of heat reservoirs and working fluid. Numerical examples for the optimal configurations with $n = -1$, n=1, n=2, n=3 and n=4 are provided, respectively.

2. Heat engine model

The following assumptions are made for the heat engine model:

1) The engine is an endoreversible one;

2) The heat conductivity between working fluid and reservoirs is ρ which subject to

$$0 \leq \rho \leq \rho_0 \tag{1}$$

3) The heat transfer between working fluid and reservoirs obeys a universal heat transfer law, the heat flux is

$$\dot{q} = \rho(T_R^n - T^n)\text{sign}(n) \tag{2}$$

where T is the absolute temperature of the working fluid, T_R is a constant temperature of each heat reservoir, and

$$T_L \leq T_R \leq T_H \tag{3}$$

where T_L and T_H are the lower and upper limits of the temperature of heat reservoirs, respectively. sign(n) is a sign function, sign(n)=1 if n>0 and sign(n)= -1 if $n < 0$.

4) The work done by the engine in one cycle is given by

$$W = \int_0^\tau P\dot{V}dt \tag{4}$$

where P and V are the pressure and volume of the working fluid, the time derivative of V is denoted by $\dot{V}$, and τ is the cycle period of the engine. The working fluid is an ideal gas.

In terms of the first law of thermodynamics for an ideal gas one has

$$C_V\dot{T} + C_V(\gamma - 1)\dot{T}\Big/V = \dot{q} \tag{5}$$

where C_V is the isometric heat capacity of the gas, γ is the ratio of isobaric heat capacity to C_V, and the time derivative of T is denoted by $\dot{T}$.

Substituting Eq. (2) into Eq. (5) and defining some new variables yields:

$$\dot{T} = -CT + \hat{K}(T_R^n - T^n)\text{sign}(n) \tag{6}$$

$$\beta = (\gamma - 1)\ln\frac{V}{V_0} \tag{7}$$

$$\dot{\beta} = C \tag{8}$$

where $\hat{\rho}$ = ρ/C_V , V_0 is a constant reference volume, and C is the change rate of cylinder volume.

In terms of these variables, Eq. (4) becomes:

$$W = C_V \int_0^\tau CTdt \tag{9}$$

Apparently, deriving β and C is convenient for solving the problem one confronts by using optimal control theory. One also has

$$Q_1 = C_V \int_0^\tau \hat{K}(T_R^n - T^n)\text{sign}(n)\theta \times [(T_R^n - T^n)\text{sign}(n)]dt \tag{10}$$

where $\theta(x)$ is a Heaviside step function, θ = 1 if $x > 0$ and θ=0 if x <0, and Q_1 is the work be supplied to system, *i.e.* input energy. The cycle efficiency is given by $\eta = W/Q_1$.

The problem now is to determine parameters $\hat{\rho}$(t), T_R(t) and $C(t)$ so that the work output is a maximum with the fixed Q_1. It is required that C be restricted such that

$$-C_m \leq C \leq C_M \tag{11}$$

where C_m and C_M are arbitrary constant positive numbers. Then the optimal cycle of the engines for maximum-efficiency can be derived by the model.

3. Optimization procedure

To determine the optimal configuration for maximum-efficiency with fixed cycle time and input energy, Q_1 is the same as in determining the optimal configuration for maximum $W - \mu Q_1$, where μ is an ordinary Lagrange multiplier. The derivation of the optimal solution is complicated by the μ term. One can show that $\mu = \partial W_{\max}/\partial Q_1$, *i.e.*, μ is a measure of the sensitivity of $W_{\max}$ with respect to small changes in the constraint, Q_1=const. One can see that μ can be both positive and negative and μ vanishes for the maximum power output, as expected [26]. To simplify the subsequent discussion, $\mu \geq$0 is assumed.

The Hamiltonian function in terms of Eqs. (6), (7), (11) and $W-\mu Q_1$ is (where T and β are called state variables and T_R, $\hat{\rho}$ and C are called control variables) is:

$$H = CT - \mu\hat{\rho}(T_R^n - T^n)\text{sign}(n) \times \theta[(T_R^n - T^n)\text{sign}(n)] + \psi_1 F_1 + \psi_2 F_2 \quad (12)$$

where

$$F_1 = -CT + \hat{K}(T_R^n - T^n)\text{sign}(n) \quad (13)$$

$$F_2 = C \quad (14)$$

Taking $(W-\mu Q_1)/C_V$ as the performance index, it is convenient to rewrite Eq. (12) as

$$H = [(1-\Psi_1)T + \Psi_2]C + (\Psi_1 - \mu\theta)\hat{\rho}(T_R^n - T^n)\text{sign}(n) \quad (15)$$

The equations of adjoint variables are given by

$$\dot{\psi}_1 = -\partial H/\partial T = -C(1-\psi_1) + n\hat{\rho}T^{n-1}(\psi_1 - \mu\theta) \quad (16)$$

$$\dot{\psi}_2 = -\partial H/\partial\beta = 0 \quad (17)$$

where

$$0 \le \hat{\rho} \le \rho_0/C_V = \hat{\rho}_0 \quad (18)$$

3.1. Application of maximum principle

Define

$$\Delta H = H[\vec{x}^*(t), \vec{u}^*(t), \vec{\psi}^*(t)] - H[\vec{x}^*(t), \vec{u}, \vec{\psi}^*(t)] \quad (19)$$

where $\vec{u}$ is an admissible solution. The asterisk of symbols state the solutions are optimal. For a maximum, it is required that ΔH$\geq$0, and thus

$$\Delta H = [(1-\psi_1^*)T^* + \psi_2^*](C^* - C) + [\psi_1^* - \mu^*\theta((T_R^{*^n} - T^{*^n})\text{sign}(n))] \times \hat{\rho}^*(T_R^{*^n} - T^{*^n})\text{sign}(n) - [\psi_1^* - \mu\theta((T_R^n - T^{*^n})\text{sign}(n))] \times \hat{\rho}(T_R^n - T^{*^n})\text{sign}(n) \ge 0 \quad (20)$$

where $0 \le \hat{\rho} \le \rho_0/C_V = \hat{\rho}_0 C_V = \hat{\rho}_0$, $T_L \le T_R \le T_H$ and -C_m $\leq$C $\leq$ C_M.

Now one can consider various possible cases separately. First set $\hat{\rho} = \hat{\rho}^*$ and $T_R = T_R^*$; then the second term of Eq. (20) vanishes. To assure $\Delta H \geq$0 it is required that

$$C^* = \begin{cases} C_M, & \text{if } (1-\psi_1^*)T* + \psi_2^* > 0 \\ -C_m, & \text{if } (1-\psi_1^*)T* + \psi_2^* < 0 \\ \text{undetermined}, & \text{if } (1-\psi_1*)T^* + \psi_2^* = 0 \end{cases} \quad (21)$$

The last possibility corresponds to what is called the "singular control problem", and for the problem it is easy to obtain that along the singular part of the trajectory C^* is constant.

Next set $C = C^*$ and $T_R = T_R^*$; then Eq. (20) yields

$$\Delta H = [\psi_1^* - \mu^*\theta((T_R^{*^n} - T^{*^n})\text{sign}(n))] \times (T_R^{*^n} - T^{*^n})\text{sign}(n)(\hat{\rho}^* - \hat{\rho}) \ge 0 \quad (22)$$

Correspondingly, it is required that

$$\hat{\rho}^* = \begin{cases} \hat{\rho_0}^* \ \text{ if } \ [\psi_1 * - \mu^*\theta((T_R^{*^n} - T^{*^n})\text{sign}(n))] \\ \quad \times (T_R^{*^n} - T^{*^n})\text{sign}(n) > 0 \\ 0 \ \text{ if } \ [\psi_1^* - \mu^*\theta((T_R^{*^n} - T^{*^n})\text{sign}(n))] \\ \quad \times (T_R^{*^n} - T^{*^n})\text{sign}(n) > 0 \\ \text{undetermined} \ \text{ if } \ [\psi_1^* - \mu^*\theta((T_R^{*^n} - T^{*^n}) \\ \times\text{sign}(n))](T_R^{*^n} - T^{*^n})\text{sign}(n) = 0 \end{cases} \quad (23)$$

The last possibility still corresponds to the singular control problem, because it would call for $\Psi_1 = \mu = 1$, further resulting in H^*=0; since this is not in agreement with the request for H^*>0, one should exclude this possibility.

Finally, set $C = C^*$ and $\hat{\rho} = \hat{\rho}^*$; then Eq. (20) yields

$$\Delta H = \begin{cases} \hat{K}^*(\psi_1^* - \mu^*)(T_R^{*^n} - T_R^n)\text{sign}(n) \\ \quad \text{if } \ T_R^* > T^* \\ \hat{K}^*\psi_1^*(T_R^{*^n} - T_R^n)\text{sign}(n) \\ \quad \text{if } \ T_R^* \le T^* \end{cases} \quad (24)$$

From Eq. (23), one can see that $\hat{\rho}^*$=$\hat{\rho_0}$ requires $\Psi_1^* > \mu^*$ if $T^* > T^*$ and Ψ_1^* <0 if $T_R^* < T^*$. Consider T_R in the interval [T^* ,T_H]; for $T_R^* > T^*$, one can find $T_R^* = T_H$ in order that ΔH >0. It then follows that $\Delta H \geq 0$ for T_R^* in the interval [T_L ,T^*], since $\mu* \geq 0$. In a similar fashion, when $T_R^* < T^*$, $\Delta H \geq$0, provided $T_R^* = T_L$. Therefore, one has

$$T_R^* = \begin{cases} T_H & \text{if } \ \psi_1^* > \mu* \\ T_L & \text{if } \ \psi_1^* < 0 \end{cases} \quad (25)$$

and for $\hat{\rho}* \neq 0$, one has $T_H > T^* > T_L$.

This problem could be changed into finding the optimal configuration for maximum-power output. If $\mu^* > 0, \hat{\rho}^* = 0$ and $C^* = C$, Eq. (20) can be changed into

$$\Delta H = -[\psi_1^* - \mu^*\theta((T_R^n - T^{*^n})\text{sign}(n))] \times \hat{\rho}(T_R^n - T^{*^n})\text{sign}(n) \ge 0 \quad (26)$$

From Eqs. (25) and (26), one can get T^*>T_H if $\psi_1^* > \mu^*$, and $T^* < T_L$ if $\psi_1^* < 0$, so that both cases are impossible. And if $0 \le \psi_1^* \le \mu^*$, T^* is possible between T_H and T_L. From the above argument, one can get that adiabatic branches may take place when $\mu^* > 0$. If $\mu^* = 0$, the [1] adiabatic branch vanished [26, 38-40]. The problem would be more complex if $\mu < 0$, when[2] the optimal configuration may be without adiabatic branches.

3.2. Optimal solutions

It is easy to find all possible optimal solutions now; one can obtain the optimal trajectories by solving the canonical functions. All functions below are optimal. It is convenient to eliminate the asterisk from the symbols.

(1) Adiabatic branches: $\hat{\rho}=0$, $C=C_M$ or $C=-C_m$

$$T(t)=T(t_0)e^{-C(t-t_0)}, \beta(t)=\beta(t_0)+C(t-t_0),$$
$$\psi_1(t)=1-[1-\psi_1(t_0)]e^{C(t-t_0)}, \quad \psi_2=\text{const} \tag{27}$$
$$H=\{[1-\psi_1(t)]T+\psi_2\}C$$
$$=\{[1-\psi_1(t_0)]T(t_0)+\psi_2\}C \tag{28}$$

where H and ψ_2 are constants as required and the value of C is determined by Eq. (21); t_0 is the initial time of the branches.

(2) Maximum-efficiency branches: $\hat{\rho}=\hat{\rho}_0$, $T_R=T_H$ or $T_R=T_L$, $C=C_M$ or $C=-C_m$

$$\dot{T}=-CT+\hat{\rho}(T^{-1}-T_R^{-1}),$$
$$\beta(t)=\beta(t_0)+C(t-t_0) \tag{29}$$
$$\dot{\psi}_1=-C(1-\psi_1)+n\hat{\rho}_0$$
$$\times[\psi_1-\mu\theta((T_R^n-T^n)\text{sign}(n))]T^{n-1},$$
$$\psi_2(t)=\text{const} \tag{30}$$

where the value of C is determined by Eq. (21) and the value of T_R is determined by Eq. (25), and t_0 is the initial time of the branches. Analytical solutions are rare, thus one has to count on numerical techniques to obtain all the solutions.

(3) Isothermal branches: $\hat{\rho}=\hat{\rho}_0$, $T_R=T_H$ or $T_R=T_L$, $(1-\psi_1)T+\psi_2=0$

$$T=T_r, \beta(t)=\beta(t_0)+C_r(t-t_0),$$
$$C_r=\frac{\hat{\rho}_0(T_R^n-T_r^n)\text{sign}(n)}{T_r} \tag{31}$$
$$\psi_1=\frac{T_R^n+T_r^n[n\mu\theta((T_R^n-T_r^n)\text{sign}(n))-1]}{T_R^n-(1-n)T_r^n},$$
$$\psi_2=\frac{-n[1-\mu\theta((T_R^n-T_r^n)\text{sign}(n))]T_r^{n+1}}{T_R^n-(1-n)T_r^n} \tag{32}$$

where T_r is a constant. This is a singular case that has not been analyzed. It is easy to prove that C, T and ψ_1 are constants by differentiating $(1-\psi_1)T+\psi_2=0$ and eliminating the derivative of time using canonical functions.

The subscript r used above corresponds to R in T_R, *i.e.* $r=h$ if $T_R=T_H$ and $r=l$ if $T_R=T_L$. The value of T_R is determined by Eq. (25). It is easy to show that

$$H=\hat{\rho}_0$$
$$\times\frac{(T_R^n-T_r^n)^2[1-\mu\theta((T_R^n-T_r^n)\text{sign}(n))]}{T_R^n-(1-n)T_r^n}\text{sign}(n) \tag{33}$$

From the fact that ψ_2 and H are constants, one has

$$\frac{(T_H^n-T_h^n)^2(1-\mu)}{T_H^n-(1-n)T_h^n}=\frac{(T_L^n-T_l^n)^2}{T_L^n-(1-n)T_l^n},$$
$$\frac{T_h^{n+1}(1-\mu)}{T_H^n-(1-n)T_h^n}=\frac{T_l^{n+1}}{T_L^n-(1-n)T_l^n} \tag{34}$$
$$C_h=\frac{\hat{\rho}_0(T_H^n-T_h^n)}{T_h}\text{sign}(n),$$
$$C_l=\frac{\hat{\rho}_0(T_L^n-T_l^n)}{T_l}\text{sign}(n) \tag{35}$$

Thus there are eight different solutions to the equations above which are presented by $1^{\pm}$, $2_H^{\pm}$, $2_L^{\pm}$, 3_H and 3_L, where the symbol "+" refers to $C=C_M$ and the symbol "-" to $C=-C_m$; the subscripts H and L correspond to the subscript of T_R. If $\mu=0$, the analytical results are the same as the optimal solutions of endoreversible heat engines for maximum-power output objective [26, 39, 40].

In order to determine the actual optimal trajectory, one must examine the constancy H and the continuity of the state variables and costate variables at switchings between pairs of optimal solutions.

3.3. Switching

The surfaces in state variable phase space across which optimal-control variables change discontinuously are called "switching surface" in optimal control theory. The switchings of the problem are summarized in Table I.

If there is a switching between branches 1^+ and 1^-, Eq. (21) requires that $(1-\psi_1)T+\psi_2$ vanish, then Eq. (28) leads to $H=0$, so there cannot be a switching between branches 1^+ and 1^-. Similarly, there is no switching between branches 3_H and 3_L because of the continuity of ψ_1.

However, there may be switchings between $T_R=T_H$ and $T_R=T_L$ in case (2), in which C remains constant and ψ_1 passes through zero at the switching time. $-C_m$ and C_M, in

TABLE I. Switchings

	1	2	3
1	①	② or ③	①
2	② or ③	④	④
3	①	④	①

① Forbidden switchings

② Allowed switchings: $\Delta C=0$ and $\Psi_1=0$

③ Allowed switchings: $\Delta C=0$ and $\Psi_1=\mu$

④ Allowed switchings: $\Delta T_R=0$, $(1-\Psi_1)T+\Psi_2=0$

which T_R remains constant and $(1-\psi_1)T+\psi_2$ vanishes. But T_R and C cannot change continuously because of H $\neq 0$.

A switching between 1^+ and 2_H^+ is allowed by increasing ψ_1 and making it across μ, and a switching between 1^+ and 2_L^+ is allowed by decreasing ψ_1 and making it across zero. The switching condition of each branch is shown below:

- The switching condition between 3_H and 2_H^+ is $[1-\psi_1(t_1)]T(t_1)+\psi_2(t_1)=0$;
- The switching condition between 2_H^+ and 1^+ is $\psi_1(t_2)=\mu$;
- The switching condition between 1^+ and 2_L^+ is $\psi_1(t_{2'})=0$;
- The switching condition between 2_L^+ and 3_L is $[1-\psi_1(t_3)]T(t_3)+\psi_2(t_3)=0$;
- The switching condition between 3_L and 2_L^- is $[1-\psi_1(t_4)]T(t_4)+\psi_2(t_4)=0$;
- The switching condition between 2_L^- and 1^- is $\psi_1(t_{5'})=0$;
- The switching condition between 1^- and 2_H^- is $\psi_1(t_5)=\mu$.

3.4. Optimal controls and trajectory

The case discussed above is an autonomous system, *i.e.*, invariant with respect to time translation, so one may choose any point along optimal trajectory as a starting point. Here one assumes that it begins from branch 3_H, *i.e.* T_R=T_H and T=T_h, etc. For $0 \le t \le t_1$, the only allowed switching is to a branch 2_H^+, *i.e.* $T_R = T_H$, $C = C_M$, etc. For $t_1 \le t \le t_2$, ψ_1 decreases and $(1-\psi_1)T+\psi_2$ increases from zero; thus the only possible transition occurs at t_2 when $\psi_1 = 0$, and one can obtain the branch $2_{\rm L}^+$. Notice that there is an adiabatic branch 1^+ between t_2 and $t_{2'}$, which is different from the optimal configuration for maximum power configuration [26,39,40].

From $t_{2'}$ to t_3, ψ_1 continues to decrease and so does $(1-\psi_1)T+\psi_2$ until it vanishes, at which time another switch becomes possible. At t_3, one begins an isothermal branch 3_L which lasts until time t_4 when one switches to branch 2_L^-. Along this branch, $(1-\psi_1)T+\psi_2$ decreases from zero while ψ_1 increases until it reaches zero at $t_{5'}$. There is also an adiabatic branch 1^- between $t_{5'}$ and t_5. Then one switches to branch 2_H^- until $(1-\psi_1)T+\psi_2$ returns to zero at the end of the cycle $t_6=\tau$.

Consequently, one can obtain the solution to the problem. Since ψ_2 is constant throughout the cycle, one records it only once. The state and costate variables are given as the following:

For $0 \le t \le t_1$:

$$T{=}T_h, C{=}C_h, \beta{=}C_h t, T_R{=}T_H, \hat{\rho}{=}\hat{\rho}_0 \tag{36}$$

$$\psi_1(t)=\frac{T_H^n+T_h^n(n\mu-1)}{T_H^n-(1-n)T_h^n},$$

$$\psi_2(t)=\frac{n(\mu-1)T_h^{n+1}}{T_H^n-(1-n)T_h^n} \tag{37}$$

For $t_1 \le t \le t_2$:

Expanding $T(t)$ with a Taylor series at t_1 gives

$$T(t)=T(t_1)+\dot{T}(t_1)(t-t_1)+{\rm O}(t-t_1) \tag{38}$$

Taking off high-order infinitely-small ${\rm O}(t-t_1)$ gives

$$T(t)\approx T(t_1)+\dot{T}(t_1)(t-t_1) \tag{39}$$

From the continuity of $T(t)$, one can obtain $T(t_1)$=T_h, and from

$$\dot{T}(t){=}{-}C_M T(t){+}\hat{\rho}_0[T_H^n(t){-}T^n(t)]{\rm sign}(n) \tag{40}$$

i.e.

$$T(t)\approx T_h+[-C_M T_h + \hat{\rho}_0(T_H^n-T_h^n){\rm sign}(n)](t-t_1) \tag{41}$$

Expanding $\psi(t)$ with Taylor series at t_1 gives

$$\psi_1(t)=\psi_1(t_1)+\dot{\psi}_1(t_1)(t-t_1)+{\rm O}(t-t_1) \tag{42}$$

From the continuity of $\psi_1(t)$, one can obtain

$$\psi_1(t)=\frac{T_H^n+T_h^n(n\mu-1)}{T_H^n-(1-n)T_h^n},$$

and from

$$\dot{\psi}_1(t)=-C_M[1-\psi_1(t)] + n\hat{\rho}_0 T^{n-1}(t)[\psi_1(t)-\mu] \tag{43}$$

one can obtain

$$\psi_1(t)\approx\frac{T_H^n+T_h^n(n\mu-1)}{T_H^n-(1-n)T_h^n} + \frac{[-nC_M T_h^n+n\hat{\rho}_0 T_h^{n-1}(T_H^n-T_h^n){\rm sign}(n)](1-\mu)}{T_H^n-(1-n)T_h^n} \times(t-t_1) \tag{44}$$

Combining all the analysis above yields

$$T(t) \approx T_h + [-C_M T_h + \hat{K}_0(T_H^n - T_h^n)\text{sign}(n)](t - t_1) \quad (45)$$

$$\psi_1(t) \approx \frac{T_H^n + T_h^n(n\mu - 1)}{T_H^n - (1-n)T_h^n} + \frac{[-nC_M T_h^n + n\hat{\rho}_0 T_h^{n-1}(T_H^n - T_h^n)\text{sign}(n)](1-\mu)}{T_H^n - (1-n)T_h^n} \times (t - t_1) \quad (46)$$

$$\beta = C_M(t - t_1) + C_h t_1, \quad T_R = T_H, \quad \hat{\rho} = \hat{\rho}_0, \quad C = C_M \quad (47)$$

From above process, the details of each branch can be obtained. The other branches of the maximum-efficiency cycle are presented in detail below:

For $t_2 \le t \le t_{2'}$:

$$T(t) = T(t_2)e^{-C_M(t-t_2)}, \quad \beta = C_M(t - t_1) + C_h t_1, \quad \psi_1(t) = 1 - (1-\mu)e^{C_M(t-t_2)}, \quad C = C_M, \quad \hat{\rho} = 0 \quad (48)$$

where

$$T(t_2) \approx T_h + [-C_M T_h + \hat{\rho}_0 \times (T_H^n - T_h^n)\text{sign}(n)](t_2 - t_1) \quad (49)$$

For $t_{2'} \le t \le t_3$:

$$T(t) \approx T(t_2)e^{-C_M(t_{2'}-t_2)} + \{-C_M T(t_2) \times e^{-C_M(t_{2'}-t_2)} + \hat{\rho}_0(T_L^n - T^n(t_2) \times e^{-nC_M(t_{2'}-t_2)})\text{sign}(n)\}(t - t_{2'}) \quad (50)$$

$$\beta = C_M(t-t_1) + C_h t_1, \psi_1(t) \approx -C_M(t-t_{2'}), \quad T_R = T_L, \quad \hat{\rho} = \hat{\rho}_0, \quad C = C_M \quad (51)$$

For $t_3 \le t \le t_4$:

$$T = T_l, \quad \beta = C_M(t_3 - t_1) + C_h t_1 + C_l(t - t_3) \quad (52)$$

$$\psi_1 = \frac{T_L^n - T_l^n}{T_L^n - (1-n)T_l^n}, \quad T_R = T_{L,} \quad \hat{\rho} = \hat{\rho}_0, \quad C = C_l \quad (53)$$

For $t_4 \le t \le t_{5'}$:

$$T(t) \approx T_l + [C_m T_l + \hat{\rho}_0(T_L^n - T_l^n)\text{sign}(n)](t - t_4) \quad (54)$$

$$\psi_1(t) \approx \frac{T_L^n - T_l^n}{T_L^n - (1-n)T_l^n} + \frac{nC_m T_l^n + n\hat{\rho}_0(T_L^n - T_l^n)T_l^{n-1}\text{sign}(n)}{T_L^n - (1-n)T_l^n}(t - t_4) \quad (55)$$

$$\beta = C_l(t_4 - t_3) + C_M(t_3 - t_1) + C_h t_1 - C_m(t - t_4), \quad T_R = T_L, \quad \hat{\rho} = \hat{\rho}_0, \quad C = -C_m \quad (56)$$

For $t_{5'} \le t \le t_5$:

$$T(t) = T(t_{5'})e^{C_m(t-t_{5'})}, \quad \beta = C_M(t_3 - t_1) + C_h t_1 + C_l(t_4 - t_3) - C_m(t - t_4), \quad \psi_1(t) = 1 - e^{-C_m(t-t_{5'})}, \quad \hat{\rho} = 0, \quad C = -C_m \quad (57)$$

where

$$T(t_{5'}) \approx T_l + [C_m T_l + \hat{\rho}_0 \times (T_L^n - T_l^n)\text{sign}(n)](t_{5'} - t_4) \quad (58)$$

For $t_5 \le t \le t_6 = \tau$:

$$T(t) = T(t_{5'})e^{C_m(t_5 - t_{5'})} + \{C_m T(t_{5'})e^{C_m(t_5-t_{5'})} + \hat{\rho}_0[T_H^n - T^n(t_{5'}) \times e^{nC_m(t_5-t_{5'})}]\text{sign}(n)\}(t - t_5) \quad (59)$$

$$\beta = C_M(t_3 - t_1) + C_h t_1 + C_l(t_4 - t_3) - C_m(t - t_4), \quad \psi_1 \approx \mu + C_m(1-\mu)(t - t_5), \quad T_R = T_H, \quad \hat{\rho} = \hat{\rho}_0, \quad C = -C_m \quad (60)$$

From the continuity of the cycle, one can obtain

$$T(t_6)=T(0), \ \ \psi_1(t_6)=\psi_1(0), \ \ \beta(t_6)=\beta(0)=0 \quad (61)$$

From the switching condition, one can obtain

$$\psi_1(t_2)=\mu, \ \ \psi_1(t_{2'})=0, \ \ \psi_1(t_{5'})=0, \ \ \psi_1(t_5)=\mu \quad (62)$$

From the fixed cycle duration one can obtain

$$t_1+(t_4 - t_3)=\tau-(\tau-t_5)-(t_5-t_{5'}) -(t_{5'} - t_4)-(t_3 - t_{2'})-(t_{2'}-t_2)-(t_2 - t_1) \quad (63)$$

From the fixed input energy, one can obtain

$$Q_1 = C_V \int_0^\tau \hat{\rho}(T_R^n - T^n)\text{sign}(n)\theta \times [(T_R^n - T^n)\text{sign}(n)]dt = \text{const} \quad (64)$$

TABLE II. Parameters vs. Q_1 with linear phenomenological heat transfer law

$T_H = 1000$ K, $T_L = 400$ K, $C_M = 8$ s^{-1}, $C_m = 38$ s^{-1}, $C_V = 5$ kJ/(kgK), $\hat{\rho}_0 = 10^7$ kgK^2/s, $\tau = 1$ s									
	$Q_1 = 8000$ kJ			$Q_1 = 10000$ kJ			$Q_1 = 12000$ kJ		
	Δ t(s)	T(K)	β	Δ t(s)	T(K)	β	Δ t(s)	T(K)	β
t_1	0.2862	730.00	1.5362	0.3944	730.00	2.1167	0.5025	730.00	2.6971
t_2	0.0887	540.03	2.2460	0.0887	540.03	2.8264	0.0887	540.03	3.4069
$t_{2'}$	0.0034	525.44	2.2734	0.0034	525.44	2.8538	0.0034	525.44	3.4343
t_3	0.1850	467.95	3.7530	0.0949	467.95	3.6128	0.0048	467.95	3.4726
t_4	0.4246	467.95	0.4590	0.4065	467.95	0.4590	0.3885	467.95	0.4590
$t_{5'}$	0.0056	547.45	0.2455	0.0056	547.45	0.2455	0.0056	547.45	0.2455
t_5	0.0007	562.64	0.2181	0.0007	562.64	0.2181	0.0007	562.64	0.2181
t_6	0.0057	730.00	0	0.0057	730.00	0	0.0057	730.00	0
μ		0.0270			0.0270			0.0270	
P		2578.3 kW			3235.3 kW			3892.2 kW	
η		0.3223			0.3235			0.3244	

TABLE III. Parameters vs. Q_1 with Newton's heat transfer law

$T_H = 1000$ K, $T_L = 400$ K, $C_M = 12.5$ s^{-1}, $C_m = 3$ s^{-1}, $C_V = 5$ kJ/(kgK), $\hat{\rho}_0 = 20$ kg/s, $\tau = 1$ s									
	$Q_1 = 6450$ kJ			$Q_1 = 6500$ kJ			$Q_1 = 6550$ kJ		
Δ t(s)	T(K)	β	Δ t(s)	T(K)	β	Δ t(s)	T(K)	β	
t_1	0.3080	931.53	0.4269	0.3082	931.53	0.4272	0.3084	931.53	0.4276
t_2	0.0219	706.18	0.7011	0.0219	706.18	0.7014	0.0219	706.18	0.7017
$t_{2'}$	0.0248	518.16	1.0107	0.0248	518.16	1.0110	0.0248	518.16	1.0113
t_3	0.0139	431.73	1.1844	0.0139	431.73	1.1841	0.0138	431.73	1.1839
t_4	0.5440	431.73	0.4308	0.5438	431.73	0.4308	0.5436	431.73	0.4308
$t_{5'}$	0.0555	468.42	0.2642	0.0555	468.42	0.2642	0.0555	468.42	0.2642
t_5	0.0275	508.66	0.1818	0.0275	508.66	0.1818	0.0275	508.66	0.1818
t_6	0.0210	931.53	0	0.0212	931.53	0	0.0215	931.53	0
μ		0.4630			0.4630			0.4630	
P		2042.8 kW			2043.2 kW			2044.6 kW	
η		0.3119			0.3142			0.3165	

Combining Eqs. (61), (62), (63), and (64) with the equations of T_h, T_l, C_h, and C_l, one can solve out numerical solutions for all the intervals of each branch, *i.e.* t_1, (t_2-t_1), $(t_{2'}-t_2)$, $(t_3-t_{2'})$, (t_4-t_3), $(t_{5'}-t_4)$, $(t_5-t_{5'})$, and $(\tau-t_5)$, as well as T_h, T_l, C_h, C_l and the Lagrange multiplier μ. Substituting them into equations in $T(t)$, one can solve out numerical solutions for all temperatures of the working fluid, *i.e.* $T(t_1), T(t_2), T(t_{2'}), T(t_3), T(t_4), T(t_{5'})$, $T(t_5)$, and $T(t_6)$. The equations are presented in detail below:

$$T_h \approx T(t_{5'})e^{C_m(t_5-t_{5'})}+\{C_mT(t_{5'})e^{C_m(t_5-t_{5'})} +\hat{\rho}_0[T_H^n-T^n(t_{5'})e^{nC_m(t_5-t_{5'})}]\text{sign}(n)\}(t_6-t_5) \quad (65)$$

$$\mu + C_m(1-\mu)(t_6-t_5)\frac{\approx [T_H^n+T_h^n(n\mu-1)]}{(T_H^n-(1-n)T_h^n)} \quad (66)$$

$$C_M(t_3-t_{2'})+C_M(t_{2'}-t_2)+C_M(t_2-t_1) +C_ht_1+C_l(t_4-t_3)-C_m(t_6-t_5) -C_m(t_5-t_{5'})-C_m(t_{5'}-t_4)=0 \quad (67)$$

$$\mu \approx \frac{T_H^n+T_h^n(n\mu-1)}{T_H^n-(1-n)T_h^n} +\frac{[-nC_MT_h^n+n\hat{\rho}_0T_h^{n-1}(T_H^n-T_h^n)\text{sign}(n)](1-\mu)}{T_H^n-(1-n)T_h^n} \times (t_2-t_1) \quad (68)$$

$$1-(1-\mu)e^{C_M(t_{2'}-t_2)}=0 \quad (69)$$

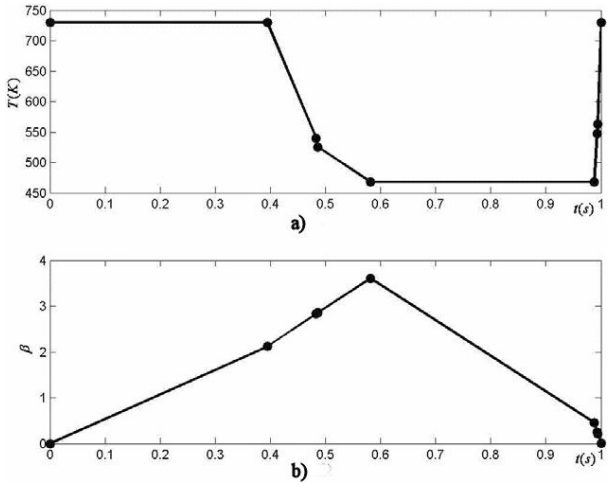

FIGURE 1. State variables for maximum efficiency objective with fixed input energy Q_1=10000 kJ and linear phenomenological heat transfer law.

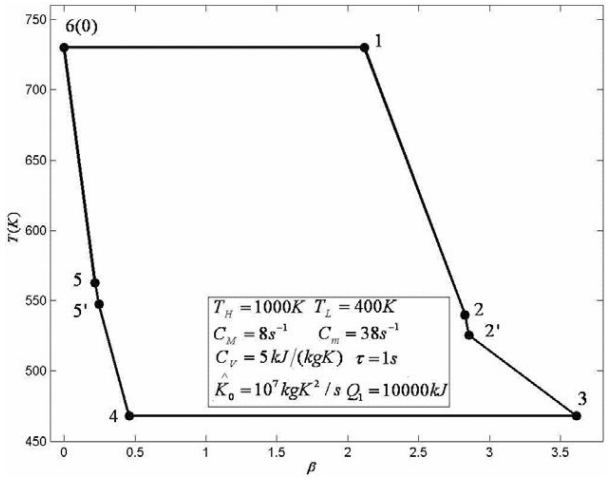

FIGURE 2. The cycle of eight branches for maximum efficiency objective with fixed input energy Q_1=10000 kJ and linear phenomenological heat transfer law.

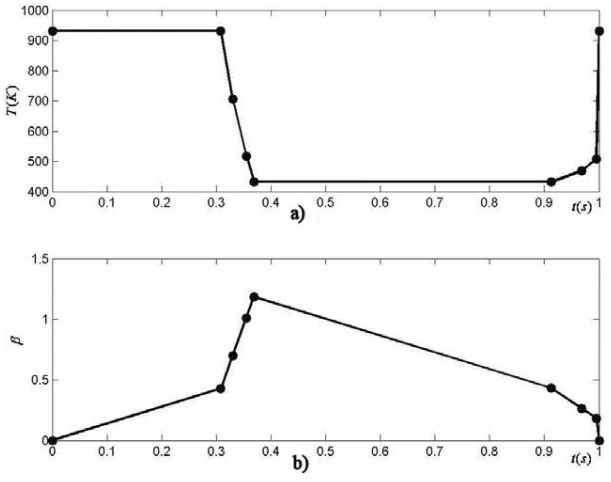

FIGURE 3. State variables for maximum efficiency objective with fixed input energy Q_1=6500kJ and Newton's heat transfer law.

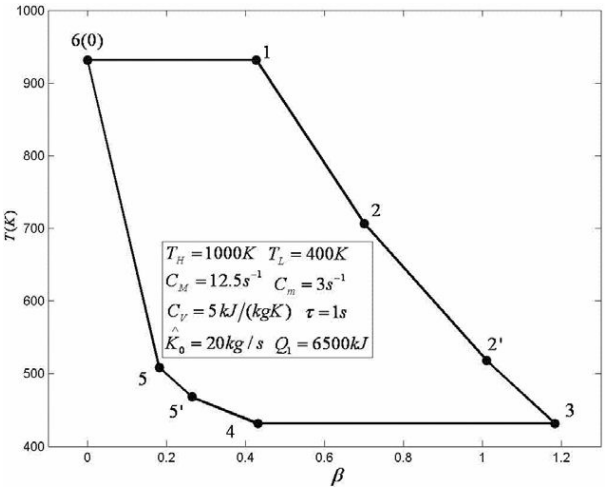

FIGURE 4. The cycle of eight branches for maximum efficiency objective with fixed input energy Q_1=6500kJ and Newton's heat transfer law.

$$0 \approx \frac{T_L^n - T_l^n}{T_L^n - (1-n)T_l^n} + \frac{nC_m T_l^n + n\hat{\rho}_0 (T_L^n - T_l^n) T_l^{n-1} \text{sign}(n)}{T_L^n - (1-n)T_l^n} (t_{5'} - t_4) \quad (70)$$

$$1 - e^{-C_m(t_5 - t_{5'})} = \mu \quad (71)$$

$$t_1 + (t_4 - t_3) = \tau - (\tau - t_5) - (t_5 - t_{5'}) - (t_{5'} - t_4) - (t_3 - t_{2'}) - (t_{2'} - t_2) - (t_2 - t_1) \quad (72)$$

$$Q_1 = C_V \int_0^\tau \hat{\rho}(T_R^n - T^n)\text{sign}(n)\theta \times [(T_R^n - T^n)\text{sign}(n)]dt = \text{ const} \quad (73)$$

$$C_h = \frac{\overset{\wedge}{0}\rho(T_H^n - T_h^n)}{T_h}\text{sign}(n) \quad (74)$$

$$C_l = \frac{\overset{\wedge}{0}\rho(T_L^n - T_l^n)}{T_l}\text{sign}(n) \quad (75)$$

$$\frac{(T_H^n - T_h^n)^2(1-\mu)}{T_H^n - (1-n)T_h^n} = \frac{(T_L^n - T_l^n)^2}{T_L^n - (1-n)T_l^n} \quad (76)$$

$$\frac{T_h^{n+1}(1-\mu)}{T_H^n - (1-n)T_h^n} = \frac{T_l^{n+1}}{T_L^n - (1-n)T_l^n} \quad (77)$$

Maximum efficiency is

$$\eta = \frac{W}{Q_1} = \frac{C_V \int_0^\tau CTdt}{Q_1} \quad (78)$$

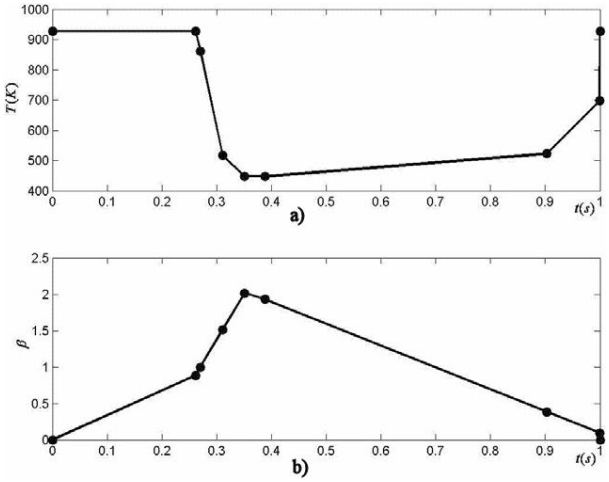

FIGURE 5. State variables for maximum efficiency objective with fixed input energy Q_1=6500kJ and square heat transfer law.

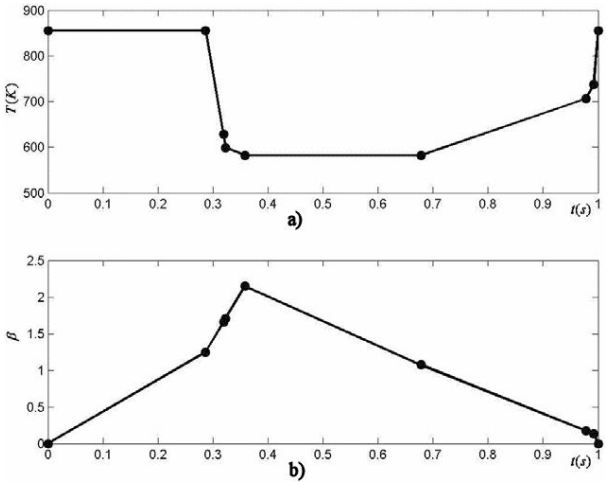

FIGURE 7. State variables for maximum efficiency objective with fixed input energy Q_1=6500 kJ and cubic heat transfer law.

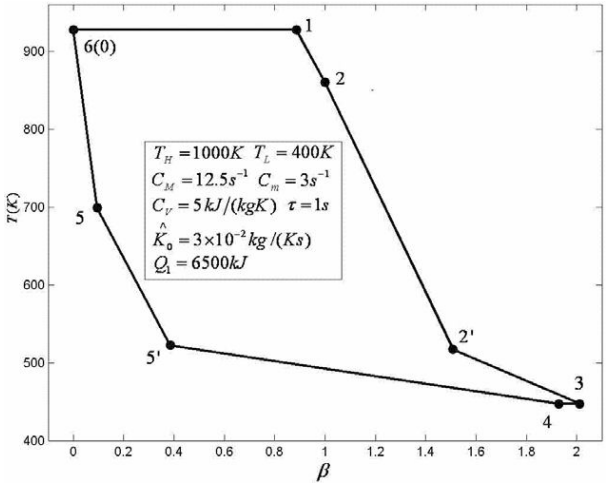

FIGURE 6. The cycle of eight branches for maximum efficiency objective with fixed input energy Q_1=6500$kJ$and square heat transfer law.

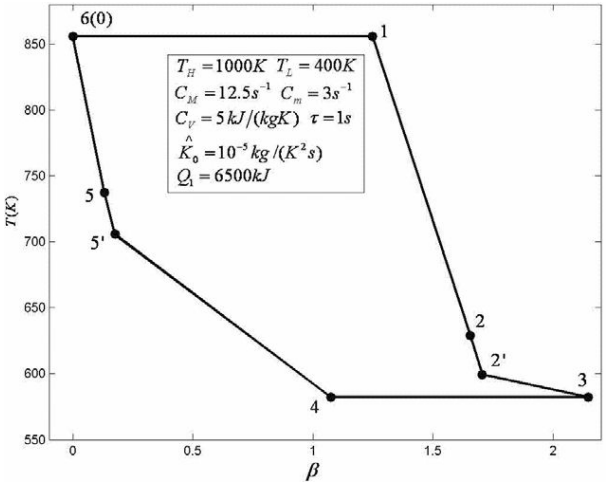

FIGURE 8. The cycle of eight branches for maximum efficiency objective with fixed input energy Q_1=6500 kJ and cubic heat transfer law.

4. Numerical Examples

Now, numerical examples for the optimal configurations of the heat engines for different heat transfer laws are provided. The results include all special heat transfer laws, such as $n=-1$, $n=1$, $n=2$, $n=3$ and $n=4$.

4.1. Optimal configuration with $n=-1$

In this case, T_H=1000K, T_L=400 K, C_M=8 s^{-1}, C_m= 38 s^{-1}, $\hat{\rho}_0$=10^7 kgK^2/s, τ=1 s, C_V=5 kJ/(kgK) and the mass of working fluid of 1kg are set. Also, sign$(n)=-1$ holds. Based on the method mentioned above, one can obtain all the numerical solutions. Table II lists the process-times of each branch, the values of the state variables at switchings, the maximum efficiency η and the corresponding power output P.

Figure 1 shows state variables for the efficiency objective with Q_1=10000 kJ. Figure 2 shows the cycle of eight branches for the maximum efficiency objective with Q_1=10000 kJ.

In this example, time is mostly spent on two isothermal branches. The change in Q_1 has an obvious influence on the intervals of two isothermal branches and the 2_L^+ branch, and has little influence on the intervals of other branches, the temperatures of working fluid at the switchings, and the Lagrange multiplier μ. It is shown that, with the increase in Q_1, the power output P and the maximum efficiency η increase, as well as the interval of 3_H branch, and the interval of 3_L branch decreases.

4.2. Optimal configuration with n=1

In this case, T_H=1000 K, T_L=400 K, C_M=100 s^{-1}, C_m=100 s^{-1}, $\hat{\rho}_0$=20 kg/s, τ=1 s, C_V=5 kJ/(kgK) , and the

TABLE IV. Parameters vs. Q_1 with square heat transfer law

$T_H = 1000$ K, $T_L = 400$ K, $C_M = 12.5$ s^{-1}, $C_m = 3$ s^{-1}, $C_V = 5$ kJ/(kgK), $\hat{\rho}_0 = 3 \times 10^{-2}$ kg/(Ks), $\tau = 1$ s									
	$Q_1 = 6450$ kJ			$Q_1 = 6500$ kJ			$Q_1 = 6550$ kJ		
	$\Delta t(s)$	$T(K)$	β	$\Delta t(s)$	$T(K)$	β	$\Delta t(s)$	$T(K)$	β
t_1	0.2770	929.31	0.8864	0.2611	927.23	0.8859	0.2632	927.90	0.8999
t_2	0.0069	877.51	0.9725	0.0091	860.30	0.9992	0.0112	844.45	1.0403
$t_{2'}$	0.0419	519.56	1.4966	0.0407	517.16	1.5081	0.0411	505.31	1.5539
t_3	0.0409	444.99	2.0073	0.0403	447.01	2.0119	0.0366	447.01	2.0117
t_4	0.0211	444.99	1.9629	0.0375	447.01	1.9280	0.0085	447.01	1.9925
$t_{5'}$	0.5153	545.23	0.4169	0.5142	522.36	0.3855	0.5397	526.02	0.3736
t_5	0.0964	728.07	0.1277	0.0970	698.76	0.0946	0.1015	713.26	0.0691
t_6	0.0126	929.31	0	0.0143	927.23	0	0.0142	927.90	0
μ		0.5942			0.5446			0.5424	
P		2520.3 kW			2565.7 kW			2592.1 kW	
η		0.3848			0.3978			0.3988	

mass of working fluid of 1 kg are set. Table III lists the process-times of each branch, the values of the state variables at switchings, the maximum efficiency η and the corresponding power output P. Figure 3 shows state variables for the maximum efficiency objective with Q_1=6500 kJ. Figure 4 shows the cycle of eight branches for the maximum efficiency objective with Q_1=6500 kJ.

4.3. Optimal configuration with n=2

In this case, T_H=1000 K, T_L=400 K, C_M=8 s^{-1}, C_m= 8 s^{-1}, $\hat{\rho}_0$=3 $\times$ 10^{-2} kg/Ks, τ=1 s, C_V=5 kJ/(kgK), and the mass of working fluid of 1 kg are set. Table IV lists the process-times of each branch, the values of the state variables at switchings, the maximum efficiency η and the corresponding power output P. Figure 5 shows state variables for the maximum efficiency objective with Q_1=6500 kJ. Figure 6 shows the cycle of eight branches for the maximum efficiency objective with Q_1=6500 kJ.

In this example, time is mostly spent on two isothermal branches. It is shown that, with the increase in $\hat{\rho}_0$, there is little influence on the temperatures of working fluid at the switchings and intervals of each branch, and the maximum power output per cycle P increases, but the corresponding efficiency η decreases.

4.4. Optimal configuration with n=3

In this case, T_H=1000 K, T_L=400 K, C_M=100 s^{-1}, C_m=100 s^{-1}, $\hat{\rho}_0 = 10^{-5}$ kg/(K^{2}s), τ=1 s, C_V=5 kJ/(kgK), and the mass of working fluid of 1 kg are set. Table V lists

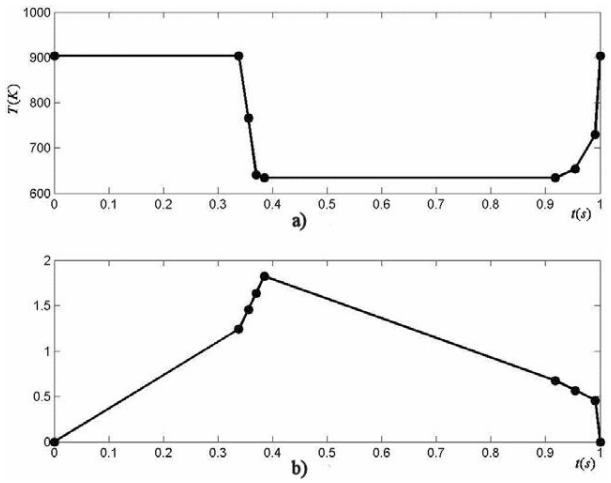

FIGURE 9. State variables for maximum efficiency objective with fixed input energy Q_1=6500 kJ and radiative heat transfer law.

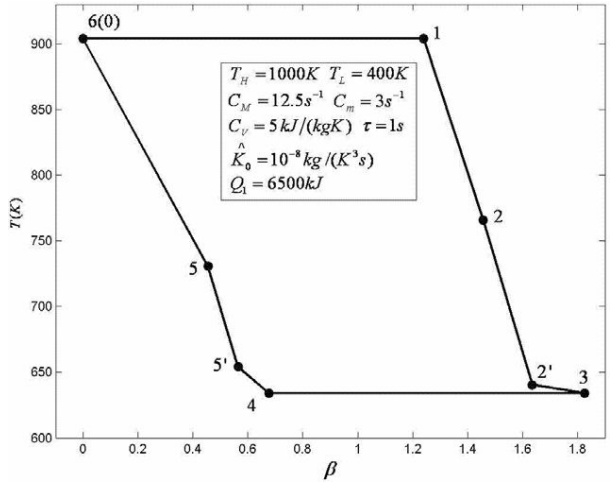

FIGURE 10. The cycle of eight branches for maximum efficiency objective with fixed input energy Q_1 = 6500 kJ and radiative heat transfer law.

TABLE V. Parameters vs. Q_1 with cubic heat transfer law

$T_H = 1000$ K, $T_L = 400$ K, $C_M = 12.5$ s^{-1}, $C_m = 3$ s^{-1}, $C_V = 5$ kJ/(kgK), $\hat{\rho}_0 = 10^{-5}$ kg/(K^{2}s), $\tau = 1$ s									
	$Q_1 = 6450$ kJ			$Q_1 = 6500$ kJ			$Q_1 = 6550$ kJ		
	$\Delta t(s)$	$T(K)$	β	$\Delta t(s)$	$T(K)$	β	$\Delta t(s)$	$T(K)$	β
t_1	0.2803	853.96	1.2367	0.2865	855.72	1.2484	0.2913	857.27	1.2550
t_2	0.0329	626.56	1.6485	0.0326	628.87	1.6557	0.0299	647.71	1.6284
$t_{2'}$	0.0054	585.53	1.7163	0.0038	599.401	1.7037	0.0074	590.68	1.7206
t_3	0.0424	586.38	2.2463	0.0355	582.30	2.1469	0.0319	574.87	2.1194
t_4	0.3332	586.38	1.1016	0.3195	582.30	1.0740	0.3153	574.87	1.0826
$t_{5'}$	0.2873	696.41	0.2396	0.2998	705.95	0.1747	0.2916	710.40	0.2079
t_5	0.0112	720.17	0.2061	0.0147	737.73	0.1306	0.0260	767.94	0.1300
t_6	0.0072	853.96	0	0.0076	855.72	0	0.0132	857.27	0
μ		0.3604			0.3717			0.4098	
P		1992.7 kW			2040.0 kW			2239.0 kW	
η		0.3042			0.3138			0.3471	

TABLE VI. Parameters vs. $Q_1$with radiative heat transfer law

$T_H = 1000$ K, $T_L = 400$K, $C_M = 12.5$ s^{-1}, $C_m = 3$ s^{-1}, $C_V = 5$ kJ/(kgK), $\hat{\rho}_0 = 10^{-8}$ kg /(K^3 s), $\tau = 1$ s									
	$Q_1 = 6450$ kJ			$Q_1 = 6500$ kJ			$Q_1 = 6550$ kJ		
	$\Delta t(s)$	$T(K)$	β	$\Delta t(s)$	$T(K)$	β	$\Delta t(s)$	$T(K)$	β
t_1	0.3378	904.00	1.2385	0.3382	904.00	1.2400	0.3386	904.00	1.2414
t_2	0.0166	771.66	1.4458	0.0173	765.71	1.4566	0.0181	759.82	1.4673
$t_{2'}$	0.0143	645.35	1.6246	0.0143	640.38	1.6354	0.0143	635.45	1.6461
t_3	0.0152	634.00	1.8146	0.0152	634.00	1.8254	0.0152	634.00	1.8361
t_4	0.5324	634.00	0.6658	0.5324	634.00	0.6766	0.5324	634.00	0.6873
$t_{5'}$	0.0370	654.08	0.5548	0.0370	654.07	0.5656	0.0370	654.06	0.5763
t_5	0.0369	730.72	0.4440	0.0369	730.63	0.4549	0.0369	730.54	0.4657
t_6	0.0151	904.00	0	0.0158	904.00	0	0.0165	904.00	0
μ		0.0137			0.0137			0.0137	
P		3139.3 kW			3166.8 kW			3193.8 kW	
η		0.4867			0.4872			0.4876	

the process-times of each branch, the values of the state variables at switchings, the maximum efficiency η and the corresponding power output P. Figure 7 shows state variables for maximum efficiency objective with Q_1=6500 kJ. Figure 8 shows the cycle of eight branches for the maximum efficiency objective with Q_1=6500 kJ. The result is similar to that with n=2.

4.5. Optimal configuration with n=4

In this case,T_H=1000 K, T_L=400 K, C_M=8 s^{-1}, C_m= 5 s^{-1}, $\hat{\rho}_0 = 10^{-8}$ kg / (K^3 s), τ=1 s, C_V=5 kJ/(kgK), and the mass of working fluid of $1kg$ are set. Table VI lists the process-times of each branch, the values of the state variables at switchings, the maximum efficiency η and the corresponding power output P with radiative heat transfer law. Figure 9 shows state variables for the maximum efficiency objective with Q_1=6500 kJ. Figure 10 shows the cycle of eight branches for maximum efficiency objective with Q_1=6500 kJ.

In this example, time is also mostly spent on two isothermal branches. The change in Q_1 has just a little influence on the intervals of each branch, the temperatures of working fluid at the most switchings and the Lagrange multiplier μ. It is shown that with the increase in Q_1, the power output P and the maximum efficiency η increase, and the temperatures of working fluid at t_2 and t_2 decrease.

4.6. Comparisons for several special heat transfer laws

For more clearer observation, one just chooses three heat transfer laws, *i.e.* the linear phenomenological heat transfer law ($\hat{\rho}_0$=10^7 kgK^2/s), Newton's heat transfer law ($\hat{\rho}_0$= 20 kg/s) and the radiative heat transfer law

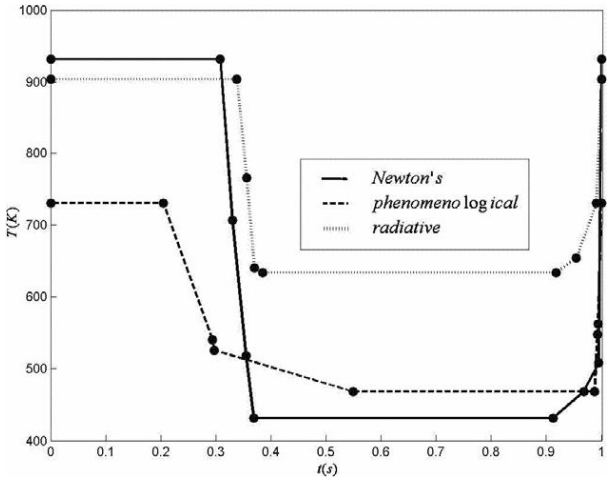

FIGURE 11. Optimal temperature of working fluid vs. time for maximum efficiency objective with three heat transfer laws.

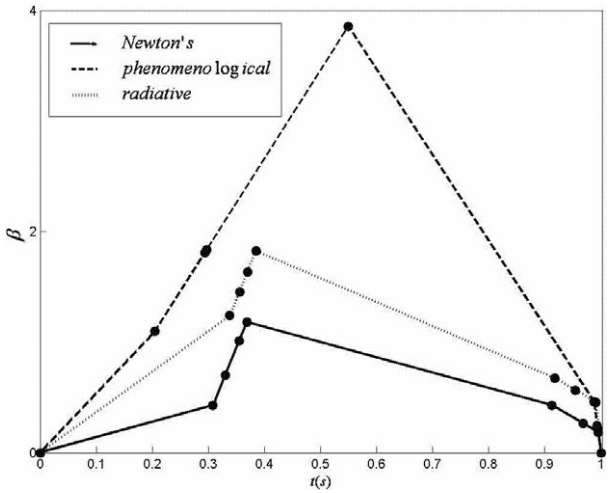

FIGURE 12. Optimal temperature of working fluid vs. time for maximum efficiency objective with three heat transfer laws.

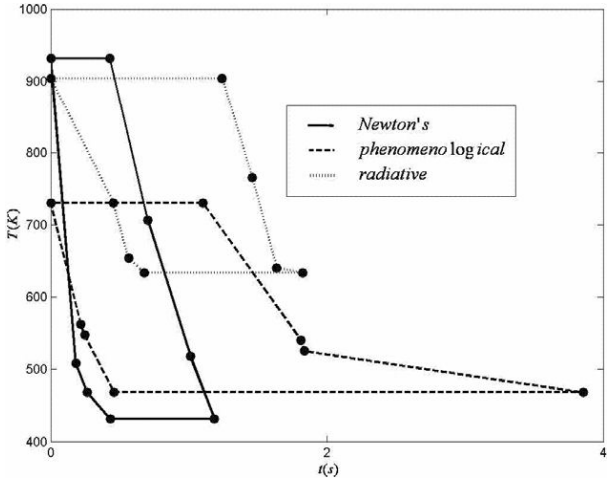

FIGURE 13. The cycles of eight branches for maximum efficiency objective with three heat transfer laws.

($\hat{\rho}_0$=10^{-8} kg/(K^3 s)), to compare. Figure 11 shows temperature of work fluid versus time with three heat transfer laws and Q_1=6500 kJ. Figure 12 shows the relative volume of the working fluid versus time with three heat transfer laws and Q_1=6500 kJ. Figure 13 shows the cycles of eight branches for maximum efficiency objective with three heat transfer laws and Q_1=6500 kJ. From Figs. 11 and 12, one can see that time is mostly spent on two isothermal branches. From Fig. 13, one can see that the optimal configurations with three heat transfer laws are obviously different from each other, so the heat transfer law has an obvious influence on the optimal configurations of the heat engines.

5. Conclusion

The optimal configuration of an endoreversible heat engine for maximum efficiency objective with fixed cycle period, fixed input energy and generalized radiative heat transfer law has eight branches including two isothermal branches, two adiabatic branches and four maximum efficiency branches which give maximum efficiency.

The similarities and differences of optimal cycles among five heat transfer laws are given as follows: the optimal cycles for five heat transfer laws all contain two isothermal branches, two adiabatic branches and four maximum-efficiency branches; for five different heat transfer laws, the temperatures of their isothermal branches are different, and the process paths of four maximum efficiency branches are different as well; the process-time is different for different branches under five different optimal configuration. Since both the process-path and the process-time are different under five different optimal configurations, the maximum efficiencies for the five configurations are different.

The results obtained can also be compared with those results of Refs. [26, 38-40] for the maximum power output objective. One can see that, because of the introduction of the Lagrange multiplier μ, the problem becomes complex, the optimal configuration changes from six branches to eight branches, and the process-path and the process-time are also different from the case of six branches. The optimal configuration is the same as the case of six branches with the same heat transfer law if and only if $\mu = 0$.

A first-order item of the Taylor series expansion was used in this paper, and the solutions would be more exact if high-order items of the Taylor series were used. In the calculations, there is only one solution for the problem if the initial values of the parameters for the calculations are located in the reasonable practical ranges.

Acknowledgements

This paper is supported by the Program for New Century Excellent Talents in University of P. R. China (Project No 20041006) and The Foundation for the Author of National Excellent Doctoral Dissertation of P. R. China (Project No. 200136).

1. B. Andresen *Finite-Time Thermodynamics*. (Physics Laboratory II, University of Copenhagen, 1983).
2. B. Andresen, P. Salamon, and R.S. Berry, *Phys. Today* (1984) 62.
3. B. Andresen, R.S. Berry, M.J. Ondrechen, and P. Salamon, (*Acc. Chem. Res.* (1984) 266.
4. S. Sieniutycz and P. Salamon, *Advances in Thermodynamics.* "Finite Time Thermodynamics and Thermoeconomics" (New York: Taylor Francis, 1990) **4**.
5. D.C. Agrawal and V.J. Menon, *Eur. J. Phys.* **11** (1990) 305.
6. D.C. Agrawal and V.J. Menon, *J. Appl. Phys.* **74** (1993) 2153.
7. D.C Agrawal, J.M Gordon, and M. Huleihil, *Indian J. Engng. Mater. Sci.* **1** (1994) 195.
8. S. Sieniutycz and J.S. Shiner, *J. Non-Equilib. Thermodyn.* (1994) 303.
9. A. Bejan, *J. Appl. Phys.* **79** (1996) 1191.
10. K.H Hoffmann, J.M Burzler, and S. Schubert, *J. Non- Equilib. Thermodyn.* **22** (1997) 311.
11. R.S Berry, V.A Kazakov, S. Sieniutycz, Z. Szwast, and A.M. Tsirlin *Thermodynamic Optimization of Finite Time Processes.* (Chichester: Wiley, 1999).
12. L. Chen, C. Wu, and F. Sun, *J. Non-Equilib. Thermodyn.* **24** (1999) 327.
13. P. Salamon, J.D. Nulton, G. Siragusa, T.R Andresen, and A. Limon *Energy, The Int. J.* **26** (2001) 307.
14. D. Ladino-Luna, *Rev. Mex. Fís.* **48** (2002) 575.
15. S. Sieniutycz, "Thermodynamic limits on production or consumption of mechanical energy in practical and industry systems." *Progress Energy Combustion Science* **29** (2003) 193.
16. K.H. Hoffman, J. Burzler, A. Fischer, M. Schaller, and S. Schubert, *J. Non-Equilib. Thermodyn.* **28** (2003) 233.
17. L. Chen, F. Sun, *Advances in Finite Time Thermodynamics: Analysis and Optimization.* (New York: Nova Science Publishers, 2004.)
18. L. Chen, *Finite time thermodynamic analysis of irreversible progresses and cycles.* (Beijing: High Education Press,(in Chinese), 2005).
19. S. Sieniutycz and H. Farkas, *Variational and Extremum Principles in Macroscopic Systems.* (London: Elsevier Science Publishers, 2005).
20. D. Ladino-Luna and R.P. Paez-Hernandez, *Rev. Mex. Fís.*, **51** (2005) 54.
21. G. Aragon-Gonzalez, A. Canales-Palma, A. Lenon-Galicia, and M. Musharrafie-Martinez, *Rev. Mex. Fís.* **51** (2005) 32.
22. C.A Herrera, M.E Rosillo, and L. Castano *Rev. Mex. Fís.* **54** (2008) 118.
23. G. Aragon-Gonzalez, A. Canales-Palma, A. Leon-Galicia, and J.R. Morales-Gomez, *Brazilian J. Physics*, **38** (2008) 1.
24. D. Cutowicz-Krusin, J. Procaccia, and J. Ross, *J. Chem. Phys.* **69** (1978) 3898.
25. F.L. Curzon , B. Ahlborn, *Am. J. Phys.* **43** (1975) 22.
26. M.H. Rubin, *Phys. Rev. A.* **19** (1979) 1272.
27. M.H. Rubin, *Phys. Rev. A.* **22** (1980) 1741.
28. A. De Vos, *Am. J. Phys.* **53** (1985) 570.
29. A. De Vos, *J. Phys. D: Appl. Phys.* **20** (1987) 232.
30. L. Chen, Z. Yan, *J. Chem. Phys.* **90** (1989) 3740.
31. J.M. Gordon, *Am. J. Phys.* **58** (1990) 370.
32. D. Ladino-Luna, *Rev. Mex. Fís.* **49** (2003) 87.
33. L. Chen, F. Sun, and C. Wu, *J. Phys. D: App. Phys.* **32** (1999) 99.
34. L. Chen, X. Zhu, F. Sun, and C. Wu, *Appl. Energy* **78** (2004) 305.
35. S. Sieniutycz, and P. Kuran, *Int. J. Heat Mass Transfer* **48** (2005) 719.
36. S. Sieniutycz, and P. Kuran, *Int. J. Heat Mass Transfer*, **49** (2006) 3264.
37. M.A. Barranco-Jimenez, N. Sanchez-Salas, and F. Angulo-Brown, *Rev. Mex. Fís.* **54** (2008) 284.
38. H. Song, L. Chen, J. Li, and C. Wu, *J. Appl. Phys.* **100** (2006) 124907.
39. H. Song, L. Chen,and F. Sun, *Appl. Energy* **84** (2007) 374.
40. J. Li, L. Chen,and F.Sun, *Applied Energy* **84** (2007) 944.
41. H.B Callen , *Thermodynamics and an Introduction to Thermostatics.* (New York: Wiley, 1985).